Biomedical Signal Processing and Control 24 (2016) 128–134

Contents lists available at ScienceDirect

Biomedical Signal Processing and Control

journal homepage: www.elsevier.com/locate/bspc

Optimal and receding horizon control of tumor growth in myeloma bone disease☆

João M. Lemos[a,*], Daniela V. Caiado[b], Rui Coelho[c], Susana Vinga[c]

[a] INESC-ID, Instituto Superior Técnico, Universidade de Lisboa, Rua Alves Redol 9, 1000-029 Lisboa, Portugal
[b] INESC-ID, Instituto Superior Técnico, Universidade de Lisboa, Lisboa, Portugal
[c] IDMEC, Instituto Superior Técnico, Universidade de Lisboa, Lisboa, Portugal

ARTICLE INFO

Article history:
Received 19 March 2015
Received in revised form 11 October 2015
Accepted 14 October 2015
Available online 8 November 2015

Keywords:
Optimal control
Receding horizon
Tumor
Bone remodeling

ABSTRACT

This article addresses the problem of designing therapies for the myeloma bone disease that optimize in a systematic way a compromise between drug toxicity and tumor repression. For that sake, the techniques of optimal control are applied to the dynamics of tumor growth, and the necessary conditions of Pontryagin's minimum principle are solved using a numerical relaxation algorithm. A therapy to accelerate bone mass recovery is applied in parallel, based on a PI control rule. Since the optimal controller provides an open-loop control, it is turned into a feedback law by following a receding horizon strategy. For that sake, an optimal manipulated variable profile is first computed over a time horizon, but only the initial part of this function is applied. The whole optimization procedure is then repeated starting at a time instant that corresponds to the end of the previously applied control.

1. Introduction

The micro-structure and evolution of the bone tissue depends of a complex process in which different cells interact through biochemical signaling substances [1]. The bone is continuously being degraded (resorption) and rebuilt, in a process called *remodeling*. In a healthy young human adult, bone formation and resorption are equilibrated along time.

The cells that are responsible for these two processes are osteoclasts and osteoblasts. Osteoblasts produce new bone by collagen synthesis and making it calcify. Opposite, osteoclasts are responsible for bone degradation. In the healthy body, the number of both types of these cells must be properly coordinated. For that sake, an important inducer of osteoclast differentiation is RANKL ([2], p. 706). When an osteoclast precursor comes in contact with RANKL molecules, this results in the maturation of an osteoclast. On the other way, osteoblasts produce also OPG that inhibits RANKL and prevents osteoclast maturation. The balance between RANKL and OPG signaling determines the degree of activation of osteoclasts and settles bone remodeling.

Cancer disrupts this balance and causes both bone disturbances and the emission of substances that favor the occurrence of metastases ([2], pp. 703–709). In particular, multiple myeloma is an hematological disease characterized by the unrelenting proliferation of plasma cells that causes destructive osteolytic lesions associated with severe pain and pathological fractures due to decreased osteoblastic and increased osteoclastic activity [3,4].

This article addresses the problem of designing therapies for the myeloma bone disease that are based on control techniques. It is stressed that the problem addressed has, as a consequence of the above remarks, an interest to cancers other then multiple myeloma. The use of optimal control allows to embed, in a systematic way, a compromise between drug toxicity and tumor repression. Furthermore, a therapy based on a PI control rule is applied in parallel to accelerate bone mass recovery.

Although optimal control provides a powerful tool to link clinical requirements to mathematical objectives, the resulting control law is open-loop, with all the inherent drawbacks. Since, in addition, some optimal drug administration profiles are such that, for a long period, the drug dose is kept at a minimum level, being only increased close to the end of the optimization time interval, this means that the patient will remain with little or no treatment at all for a significant period of time. To circumvent this problem [13], proposes to split the optimization interval in two parts.

☆ This work was supported by Fundação de Ciência e Tecnologia (Portugal) under contracts EXPL/EMSSIS/1954/2013 (CancerSys), PTDC/EMS-SIS/0642/2014 (PERDEIDS), and UID/CEC/50021/2013.

* Corresponding author. Tel.: +351 213 100 322; fax: +351 213 145 843.
E-mail addresses: jlml@inesc-id.pt (J.M. Lemos), daniela.caiado@ist.utl.pt (D.V. Caiado), rui.coelho@tecnico.ulisboa.pt (R. Coelho), susanavinga@tecnico.ulisboa.pt (S. Vinga).

http://dx.doi.org/10.1016/j.bspc.2015.10.004
1746-8094/

To tackle the above problems, this article examines the possibility of using a receding horizon (RH) strategy [17], in which, at a given time t, an optimal control problem is solved in the time horizon between t and $t+T$, called the prediction horizon. Of the resulting control function, only the part between t and $t+\delta$ is actually used, with the whole procedure being repeated starting at $t+\delta$. This procedure has the advantage of performing a feedback action every δ units of time. Usually, RH control is considered in the framework of discrete-time predictive control [18]. Since the samples of the manipulated variable along the prediction horizon are left free, in nonlinear problems they can be stuck atlocal minima. In this paper, instead, Pontryagin's minimum principle is used to select them. Although the idea of using Pontryagin's principle together with RH control is not new [19,20], this approach is rather unexplored, and has not been previously considered for tumor growth control.

The contribution of this article consists therefore of the application of a receding horizon controller based on optimal control to the design of therapies for cancer that involves an interaction between bone remodeling and tumor growth.

The paper is organized as follows: After this introduction, a brief literature review is made in Section 2, and the tumor growth models considered are described in Section 3. Pontryagin's minimum principle (PMP) is reviewed in Section 4, together with a numerical solution algorithm for optimal control problems and application examples related to the control of tumor growth. Section 5 formulates the RH algorithm based on PMP and shows results on tumor growth, and in Section 6 the PI controller for the bone mass regulation is designed. Finally, Section 7 draws conclusions.

2. Literature review

The above process of bone remodeling can be represented by mathematical models that address both physiological and pathological situations. While many articles have been published addressing a variety of situations, we only cite here [5]. In this work, a lumped nonlinear state-space model, with state variables given by the number of osteoclasts and osteoblasts, has been developed, being able to predict a number of behaviors actually observed in patients, including nonlinear oscillations.

The above model has been extended in [6] for the myeloma bone disease, including the tumor size in the state and therapeutic drug administration as manipulated variables.

Although in [7] it has been pointed out, in a context other than cancer, that the bone remodeling problem can be envisaged as an optimal control problem, cancer in relation to this process has not yet been the subject of studies to design therapies based on the systematic application of control methods. Existing studies like [5,6,8] only exploit simulations under different scenarios, but without any reference to feedback or optimal control. On the other way, there is a rich bibliography on the design of therapies for tumor repression, some addressing the bone marrow, of which [9–14] are some examples. However, the interplay between bone remodeling and tumor evolution is not considered in this bibliography, despite this interaction being more and more recognized of upmost importance for several types of cancer. Indeed, as described in [2], p. 703, it has been observed that carcinomas of the lung, breast and prostate show a strong tendency to metastasize to the bone.

3. Bone remodeling and tumor growth dynamics

The model used for the simulation study in this paper corresponds to the one described in [5,6], with slight modifications. These modifications consist in the way that the drug affects the tumor growth equation, and also in the way the drugs affect the remodeling part of the model.

3.1. Bone remodeling model

The bone remodeling process involves the activity of osteoclasts, which are cells that breakdown the bone in a process called bone resorption, and osteoblasts, that are responsible for bone formation. The mathematical model that expresses the dynamic interaction between osteoclasts $C(t)$ and osteoblasts $B(t)$, described in [5], uses normalized variables and is

$$\dot{C}(t) = \alpha_1\, C(t)^{g_{11}} B(t)^{g_{21}} - \beta_1\, C(t), \tag{1}$$

$$\dot{B}(t) = \alpha_2\, C(t)^{g_{12}} B(t)^{g_{22}} - \beta_2\, B(t), \tag{2}$$

where the dot denotes derivative with respect to time, parameters α_i and β_i, with $i=1,2$, represent the activity of cell production and removal, and parameters g_{ij}, with $i,j=1,2$ describe the net effect of all the factors that are involved in osteoclasts and osteoblasts formation. For instance, the effect of all the factors produced by osteoclasts that regulate its own production are expressed by the parameter g_{11}, referred as autocrine regulation, while parameter g_{12} express the regulation of osteoclasts in the production of osteoblasts, referred as paracrine regulation. Conversely, parameters g_{21} and g_{22} are the paracrine and autocrine regulation, respectively, of all the factors produced by osteoblasts. In this model, the parameter g_{11} is responsible for the oscillatory mode of the bone remodeling process [5].

The bone mass $Z(t)$ is modeled by

$$\dot{Z}(t) = -\kappa_1\, C^*(t) + \kappa_2\, B^*(t), \tag{3}$$

where parameters k_i, for $i=1,2$, are the normalized activity of bone resorption and bone formation constants. In (3), the number of cells Y^* (with Y denoting either C or B) is given by

$$Y^*(t) = \begin{cases} Y(t) - Y_e & \text{if } Y(t) > Y_e, \\ 0 & \text{if } Y(t) \le Y_e, \end{cases} \tag{4}$$

where Y_e is the steady state of $\dot{Y}(t)$.

In the presence of bone pathologies, the bone remodeling dynamics is disrupted. In [6], the tumor size, $X(t)$, dynamics is incorporated in the bone remodeling process, and the osteoclasts and osteoblasts dynamics are described by

$$\dot{C}(t) = \alpha_1\, C(t)^{g_{11}\left(1+r_{11}\frac{X(t)}{L}\right)} B(t)^{g_{21}\left(1+r_{21}\frac{X(t)}{L}\right)} - \beta_1\, C(t), \tag{5}$$

$$\dot{B}(t) = \alpha_2\, C(t)^{g_{12}/(1+r_{11}\frac{X(t)}{L})} B(t)^{g_{22}-r_{22}\frac{X(t)}{L}} - \beta_2\, B(t), \tag{6}$$

where L and r_{ij}, with $i,j=1,2$, are nonnegative parameters.

The steady state solution of (5) and (6) is given by

$$C_e = \left(\frac{\beta_1}{\alpha_1}\right)^{\frac{1-(g_{22}-r_{22})}{\Delta}} \left(\frac{\beta_2}{\alpha_2}\right)^{\frac{g_{21}(1-r_{21})}{\Delta}}, \tag{7}$$

$$B_e = \left(\frac{\beta_1}{\alpha_1}\right)^{\frac{g_{12}}{(1+r_{12})\Delta}} \left(\frac{\beta_2}{\alpha_2}\right)^{\frac{1-g_{11}(1+r_{11})}{\Delta}}, \tag{8}$$

where

$$\Delta = \frac{g_{12}\, g_{21}(1-r_{21})}{1+r_{12}} - (1-g_{11}(1+r_{11}))(1-g_{22}+r_{22}), \tag{9}$$

and it is assumed that X is also in its steady state. This paper considers the bone remodeling dynamics in the presence of a tumor ((3)–(6)), as described in [6].

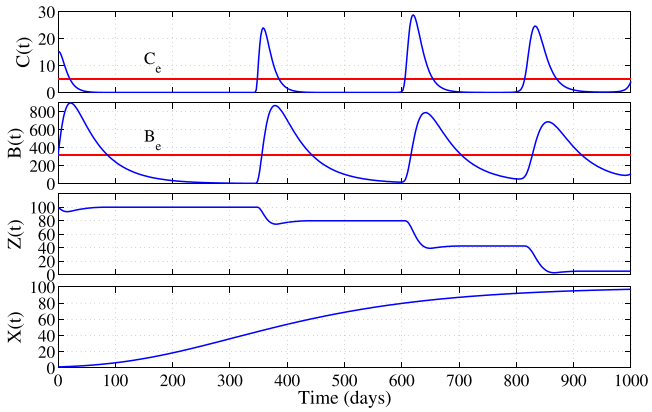

Fig. 1. Bone remodeling dynamics in the presence of tumor growth.

3.2. Tumor growth models and therapies

Let $X \in \mathbb{R}$ be a function of time that reflects the size of a tumor. The Gompertz model [12] for the evolution of X is

$$\dot{X}(t) = \gamma X(t) \log\left(\frac{L}{X(t)}\right) - \epsilon_1 u(t) X(t), \tag{10}$$

where γ, ϵ_1 and L are positive parameters.

In the absence of treatment, model (10) leads to an S-shaped growth, with X tending to L when time increases. Fig. 1 shows the tumor growth dynamics and the bone remodeling dynamics.

The bone remodeling model parameters chosen are in accordance with [6,5]. The bone cell formation constant rates assume values of $\alpha_1 = 3$ cells/day and $\alpha_2 = 4$ cells/day, and the bone cell removal constant rates take values of $\beta_1 = 0.2\,\text{day}^{-1}$ and $\beta_2 = 0.02\,\text{day}^{-1}$. The autocrine and paracrine parameters take values of $g_{11} = 1.1, g_{22} = 0, g_{12} = 1$ and $g_{21} = -0.5$. The parameters r_{ij} take values of $r_{11} = 0.005, r_{22} = 0.2, r_{12} = 0$ and $r_{21} = 0$. The constants of the normalized activity of the bone formation and resorption assume values of $k_1 = 0.0748\,\text{cell}^{-1}\,\text{day}^{-1}$ and $k_2 = 3.22 \times 10^{-4}\,\text{cell}^{-1}\,\text{day}^{-1}$. The initial values are $C(0) = 15$, $B(0) = 316$ and $X(0) = 1$ in normalized units. The tumor growth model assume values of $\gamma = 0.005$ and $L = 100$.

The manipulated variable u, assumed to be positive, also causes a decrease on the rate of growth of X. However, when X becomes small, the effect of u also decreases and there is no danger that X is driven to negative values.

Two therapies are considered. One has the function of killing the tumor cells and corresponds to the manipulated variable $u(t)$ in (10), being obtained with an optimal control law.

A second therapy is considered where *bisphosphonates* are administered to suppress the production of osteoclasts. This therapy is associated to the variable $v(t)$. Therefore (5) becomes

$$\dot{C}(t) = \alpha_1 C(t)^{g_{11}\left(1+r_{11}\frac{X(t)}{L}\right)} B(t)^{g_{21}\left(1+r_{21}\frac{X(t)}{L}\right)} - (\beta_1 + \epsilon_2 v(t)) C(t), \tag{11}$$

where ϵ_2 is a nonnegative parameter. The design of this therapy is formulated as a regulation problem that is to be solved with a proportional-integral (PI) controller that drives the bone mass to a prescribed value that is close to the healthy situation.

4. Optimal control of the tumor size

In this section the optimal controller for the tumor growth suppression is designed.

Assume that there is a period of time t, between $t = 0$ and $t = T$, in which a therapy is to be specified, in the form of a function $u : [0, T] \to \mathbb{R}$. The parameter T is called the optimization horizon.

When designing such a function, two conflicting objectives have to be considered. First, the tumor size X is to be driven to a small value, an objective that demands high values of u. Second, the toxicity, that is a function of the cumulative drug dose applied, is to be minimized, an objective that calls for small values of u. Both these objectives are expressed in mathematical terms in a cost functional to be minimized. The following quadratic cost functional is therefore considered

$$J = \int_0^T [X(t)^2 + \rho u(t)^2]\, dt, \tag{12}$$

where $\rho > 0$ is a parameter that defines the balance between both conflicting objectives. The quadratic cost assumes that the toxic effects of the therapy are proportional to u^2.

4.1. Pontryagin's minimum principle

Consider the following generic optimal control problem:

Problem 1. Let

$$\dot{X} = f(X, u), \quad X(t_0) = X_0, \tag{13}$$

with $X \in \mathbb{R}^n$, $t \in [0, T]$, with T constant and, for each t, $u \in U \subset \mathbb{R}$, where U is a convex set of admissible control values. It is assumed that there is one and only one solution to (13).

Find u such as to minimize the cost

$$J = \Psi(X(T)) + \rho \int_0^T L(X, u)\, dt, \tag{14}$$

with Ψ and L given functions that satisfy adequate assumptions convexity so that the problem has a solution.

A set of necessary conditions satisfied by the solution of *Problem 1* is given by

Pontryagin's minimum principle [15]

Along an optimal trajectory for X, u and λ, the following necessary conditions for the solution of *Problem 1* are verified:

- The state X and u verify the state equation (13), with the prescribed initial condition.
- The co-state λ verifies the adjoint equation

$$-\dot{\lambda} = \lambda^T f_X(X, u) + L_X(X, u), \tag{15}$$

with the terminal condition

$$\lambda(T) = \Psi_X(X)|_{X=X(T)}. \tag{16}$$

- For each t, the Hamiltonian function, defined by

$$H(\lambda, X, t) = \lambda^T f(X, u) + L(X, u), \tag{17}$$

is minimum with respect to u.

In (15), the following notation is used with i the line index and j the column index

$$f_X(X, u) = \left[\frac{\partial f_i}{\partial X_j}\right], \quad L_X = \left[\frac{\partial L}{\partial X_j}\right], \quad \Psi_X = \left[\frac{\partial \Psi}{\partial X_j}\right]. \tag{18}$$

4.2. Numerical solution

When considering the Gompertz model it is not possible to obtain the optimal control law in an analytical way. A possibility is to use the following numerical relaxation algorithm

Algorithm A1. Divide the time interval between $t = 0$ and $t = T$ into N subintervals of duration $\Delta t = T/N$. Let $t_i = (i - 1)\Delta t$, $i = 1, \ldots, N + 1$. To each t_i associate a value u_i and let the linear interpolation of these values in each subinterval define the control function.

Recursively execute the following steps:

1. For $i=1,\ldots,N+1$ select an initial guess of the optimal control, u_i. Set the iteration counter $K=0$.
2. Solve forward (from $t=0$ to $t=T$) the state equation (13) with the initial condition x_0 and the control that results from the interpolation of the u_i^K.
3. Solve backwards (from $t=T$ to $t=0$) the adjoint equation (15) with the terminal condition (16).
4. For $i=1,\ldots,N+1$ update the vector of optimal control approximations by

$$u_i^{K+1} = \arg\min_{v}(H(\lambda(t_i), x(t_i), v)) \tag{19}$$

subject to $u_i^{K+1} \in U, \forall i$.
5. Set $K=K+1$ and go to step *2.* until convergence is met.

Steps *2.* and *3.* are solved with an appropriate ordinary differential equation solver. In the examples reported in the next section, MATLAB `ode45` with variable step-size and precision of 10^{-16} has been used. For step *4.* the `cvx` MATLAB interface has been used [16].

4.3. Gompertz model with quadratic cost

Considering the Gompertz model (10) with the quadratic cost (12), the Hamiltonian function becomes

$$H = \lambda\,\gamma X \log\left(\frac{L}{X}\right) + X^2 - \epsilon_1\,\lambda\,X\,u + \rho\,u^2, \tag{20}$$

and, from

$$\frac{\partial H}{\partial u} = 0, \tag{21}$$

its minimum is

$$u^*(t) = \frac{\epsilon_1\,\lambda(t)X(t)}{2\,\rho}, \tag{22}$$

that is the optimal control law. The computation by (21) of the minimum with respect to u of the Hamiltonian function assumes that the minimum is an interior point of the set of admissible control values U. This assumption has to be checked *a posteriori*. If the minimum occurs at the boundary of U, one must resort to a minimization algorithm. The package `cvx` [16] can be used in this problem. The advantage of using the closed formula (22) is its faster computational speed.

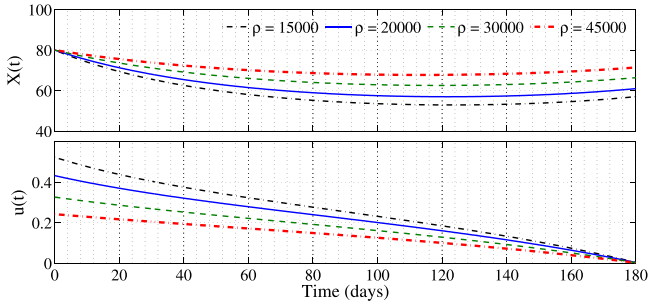

Fig. 2. Optimal control performance for an horizon of $T=180$. Effect of the parameter ρ.

Fig. 2 provides the optimal control law for an horizon of $T=180$ days, for different values of ρ, showing that, for smaller values of ρ, the drug dose increases, while the tumor size decreases. The final value of u is always zero since, at every t, this variable is proportional to λ, and $\lambda(T)=0$. As a consequence, $X(t)$ increases when t approaches T. This situation could be changed by modifying the cost in a way that imposes a penalty on the final tumor size $X(T)$. From (16) it is concluded that neither $\lambda(T)$ nor $u(T)$ would no longer vanish. In this simulation, the parameter ϵ_1 has the value of 0.018 and $X(0)=80$.

Fig. 3 illustrates the effect of parameter ρ. When ρ increases, more importance is given to the toxicity term, associated to u, in (12). Hence, the cumulative drug dose applied during the whole horizon, $P(T)$, decreases when ρ increases. The price to pay is that, consequently, the final tumor size $X(T)$ increases.

Figs. 4–6 show a sensitivity study of the results obtained with optimal control when the parameters of the Gompertz model (10) have values that are different from the ones assumed when performing control design. Fig. 4 shows the time evolution of the tumor size X, where the optimal control u computed with the nominal parameter is applied to the model with values of the parameters

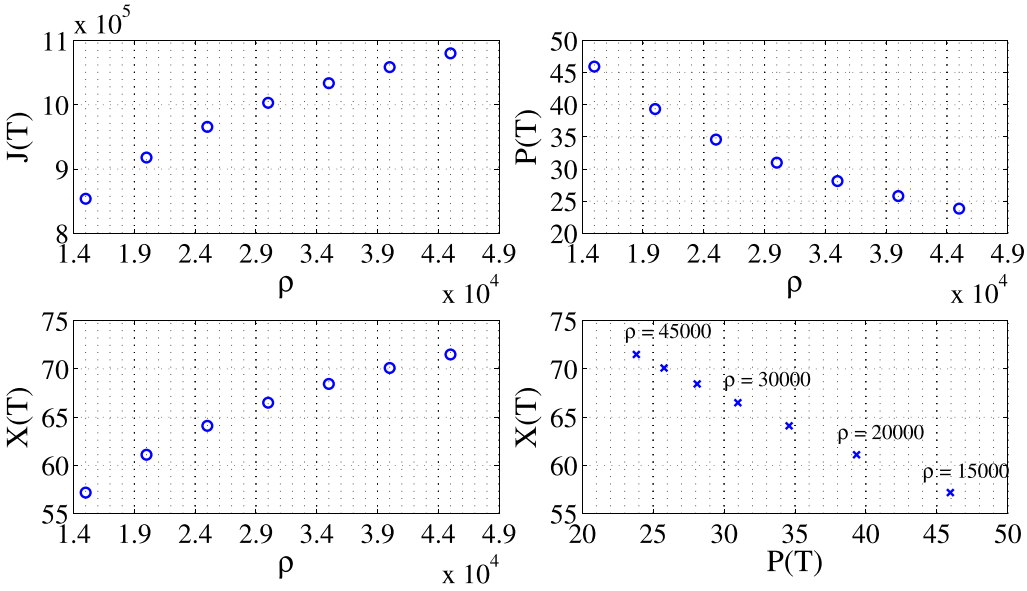

Fig. 3. Effect of the parameter ρ of the cost functional on the O.C. law, for an horizon of $T=180$ days. The final cost functional $J(T)$ and the cumulative drug dose $P(T)$ are plotted on the top two plots and the final tumor size $X(T)$ is plotted on the left bottom plot, as functions of the parameter ρ. The final tumor size is plotted as a function of the cumulative drug dose, for each ρ, on the right bottom plot.

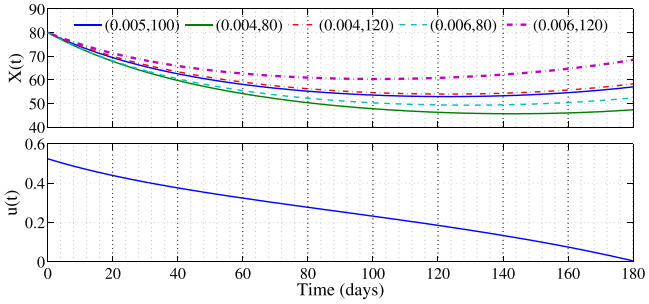

Fig. 4. Tumor evolution of X when the optimal control is designed for the nominal values of the parameters γ and L.

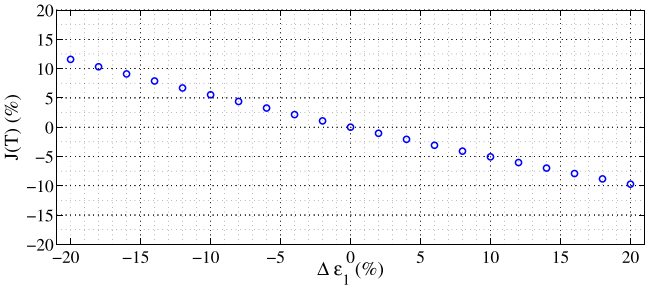

Fig. 5. Change of the cost as a function of changes of ϵ_1 when the optimal control is designed for the nominal value of the parameter.

that vary with respect to the nominal ones. Figs. 5 and 6 show similar results for the parameter ϵ_1. The sensitivity of the cost with respect to $\Delta\epsilon_1$ is approximately linear, as shown in Figs. 5 and 6 show the time evolution of the tumor when ϵ_1 assumes different values, but always using the nominal value in controller design.

5. Receding horizon control

In order to overcome the drawbacks of open-loop control, this section proposes the combination of the optimal control with a receding horizon (RH) strategy [17].

The numerical approximation of the optimal control obtained from Algorithm A1 can be recast in a RH framework as follows.

Algorithm A2. At time t, recursively compute the following steps:

1. Solve the optimal control problem with $x_0 = x(t)$ (the state at time t) as initial condition, from t to $t+T$, using Algorithm A1.
2. Apply to the system the optimal control approximation obtained in step *1.*, from t to $t+\delta$.
3. Make $t \leftarrow t+\delta$ and go to step *1.*

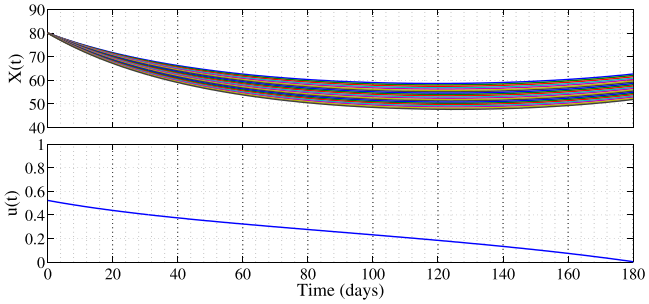

Fig. 6. Time evolution of X for different values of parameter ϵ_1, when the optimal control is designed for the nominal parameters.

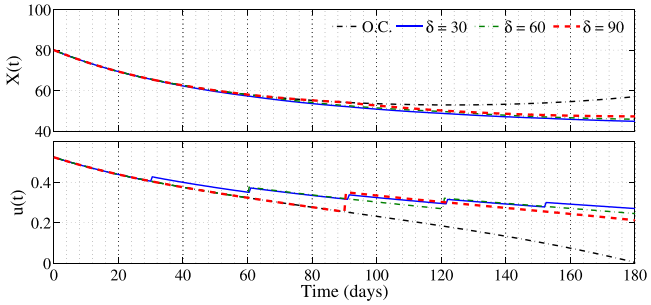

Fig. 7. RH control for different values of δ and the optimal control (O.C.) for the same horizon $T = 180$ days.

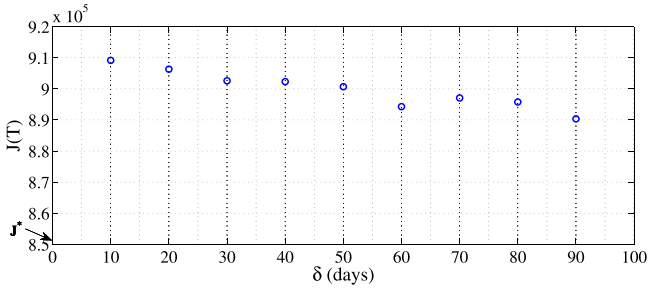

Fig. 8. Quadratic cost of the RH control for different values of δ, with an horizon of $T = 180$ days. The optimal control J^* is indicated by the arrow.

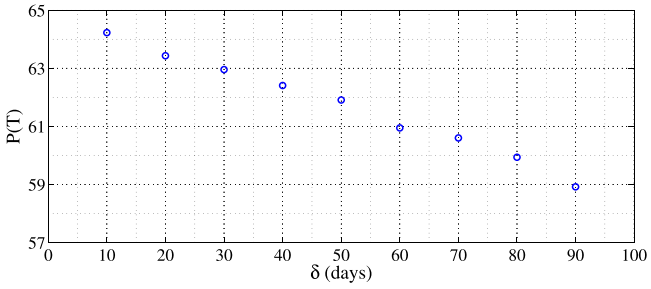

Fig. 9. Cumulative drug dose applied, $P(T)$, for different values of δ, with an horizon of $T = 180$ days.

5.1. Gompertz model with quadratic cost

Figs. 7–9 compare the optimal control with RH control for different values of δ.

As shown in Fig. 7, close to $t = T$, RH control does not drastically reduce the dose as happens with the optimal law, and decreases the final tumor size. For optimal control this drawback can be circumvented by using a convinient terminal cost. However, the optimal

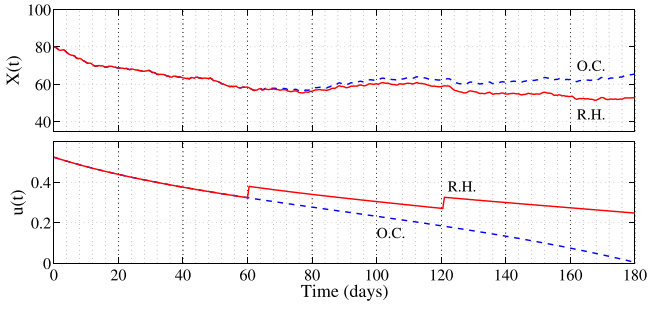

Fig. 10. RH closed-loop control performance for an horizon of $T = 180$ days and $\delta = 60$ days, in the presence of disturbances. The optimal control (O.C.) for the same horizon is also plotted.

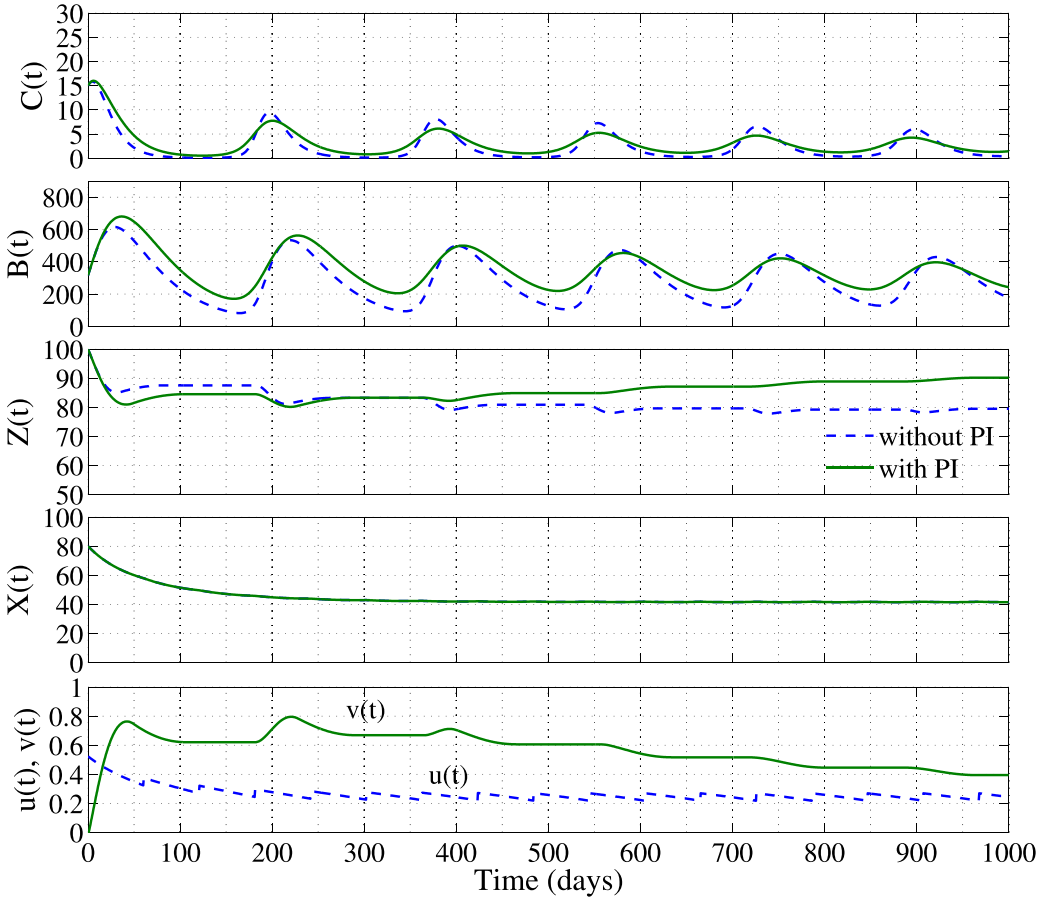

Fig. 11. Bone remodeling and tumor growth dynamics with (solid lines) and without (dashed lines) the PI controller for bone mass regulation.

control is designed for a horizon of fixed length. If the control action is to be kept for a indefinite period of time, it is better to use RH control. Another advantage of RH control with respect to optimal control is that RH control provides a feedback action since it is able to update the state variables in order to reject disturbances. Figs. 8 and 9 show the decreasing cost and cumulative drug dose as δ increases. The highest lower bound of the cost is, of course, the one obtained for $\delta = T$.

Fig. 10 illustrates the capacity of the RH control to reject a disturbance, in contrast with the optimal controller. In the simulation reported in Fig. 8, a stochastic disturbance has been added to the Gompertz model. This disturbance may correspond to a modeling error, either due to a model/controller parameter mismatch, or associated with unmodeled dynamics. The disturbance model has been selected merely for exemplificative purposes, and corresponds to a sequence of independent random variables with a Gaussian distribution, with zero mean and variance 2, with a sampling interval of 0.5 days, that is passed by a filter with transfer function

$$F_n(s) = \frac{0.5}{s + 0.5}. \tag{23}$$

When the optimal controller is used, no corrective actions to counteract the disturbance are taken because the manipulated variable is computed off-line, in a blind way. Instead, when using RH control there is a feedback associated to the measure of tumor size that influences the initial condition of the computation every $\delta = 60$ days. As a consequence, RH control is able to counteract the disturbance and leads to a smaller tumor size.

6. PI control for bone mass regulation

If the tumor size is reduced due to the specific therapy that is dosed by the optimal controller, the bone mass will increase, but very slowly. In order to speed-up bone mass recovery, a PI controller for the bone mass regulation is presented in this section. In this case it is considered that the optimal control law for the tumor growth is applied to the system and that a PI controller is used to suppress the osteoclast production by scheduling an adequate therapy. The PI controller is designed to track the error $e(t)$ between the desired value of the bone mass (100%) and the measured bone mass $Z(t)$, and to compute the appropriate drug dose $v(t)$ in order to prevent the bone mass resorption from the osteoclasts. The control signal is the drug dose $v(t)$, which is applied in (7), and is defined by

$$v(t) = K_p\, e(t) + K_i \int_0^T e(t)\, dt. \tag{24}$$

Fig. 11 shows the effect of a PI controller with $K_p = 0.01$ and $K_i = 0.02$, for $\epsilon_2 = 0.03$, applied to the system with the RH controller designed for $T = 180$ days and $\delta = 60$ days for the tumor growth control. The PI controller is able to drive the bone mass to the desired value faster than without PI control. The controller action $v(t)$ suppresses the osteoclasts production that leads to higher values of the bone mass.

7. Conclusions

The combination of optimal and receding horizon control provides a natural framework to obtain therapies for tumor growth, that was complemented with a PI controller for bone therapy.

Optimizing the therapy can be readily formulated as an optimal control problem, whose solution yields a time profile for drug administration. This open-loop solution can be transformed into a feedback control law, with all the inherent advantages, by using the receding horizon strategy. In the example provided, RH improves control performance with respect to the open-loop optimal control in the presence of disturbances.

A number of important issues were not addressed in this paper. The first one is drug resistance and multi-drug treatment.

Other aspects are related to improving the model in what concerns drug administration, and they comprise the inclusion of pharmacokinetic drug models, modeling the fact that drugs have no effect below some threshold, and the fact that drugs are not continuously perfused in the patient but instead are administered in concentrated time doses that are best represented as a sequence of impulses.

Although the above aspects are essential when modeling a realistic therapy of cancer, they exceed the objective of this paper that was circumscribed to make a first illustration of how the receding horizon can be applied to cell-kill strategies to turn an optimal profile into a feedback control law, and complement it with a PI controller to moderate osteoclast excessive action and speed-up bone mass recovery.

References

[1] A.M. Parfitt, Osteonal and hemi-osteonal remodeling: the spatial and temporal framework for signal traffic in adult bone, J. Cell. Biochem. 55 (1994) 273–286.
[2] R.A. Weinberg, The Biology of Cancer, 2nd ed., Garland Science, 2014.
[3] M.S. Raab, K. Podar, I. Breitkrentz, P.G. Richardson, K.C. Anderson, Multiple myeloma, Lancet 374 (2009) 324–339.
[4] M.R. Reagan, L. Liaw, C.J. Rosen, I. Ghobrial, Dynamic interplay between bone and multiple myeloma: emerging role of the osteoblast, Bone 75 (2015) 161–169.
[5] S.V. Komarova, R.J. Smith, S.J. Dixon, S.M. Sims, L.M. Wahl, Mathematical model predicts a critical role for osteoclast autocrine regulation in the control of bone remodeling, Bone 33 (2003) 206–215.
[6] B.P. Ayati, C.M. Edwards, G.F. Webb, J.P. Wikswo, A mathematical model of bone remodeling dynamics for normal bone cell populations and myeloma bone disease, Biol. Direct 5 (2010) 28.
[7] T. Lekszycki, Functional adaptation of bone as an adaptive control problem, J. Theor. Appl. Mech. 43 (3) (2005) 555–574.
[8] S. Maldonado, S. Borchers, R. Findeisen, F. Allgöwer, Mathematical modeling and analysis of force induced bone growth, in: Proc. 28th IEEE EMBS Int. Conf., New York, 2006, pp. 3154–3157.
[9] M. Kimmel, A. Swierniak, Control theory approach to cancer chemotherapy: benefiting from phase dependence and overcoming drug resistance, in: A. Friedman (Ed.), Tutorials in Mathematical Biosciences III – Cell Cycle, Proliferation, and Cancer, Springer, 2006.
[10] G.W. Swan, Role of optimal control theory in cancer chemotherapy, Math. Biosci. 101 (1990) 237–284.
[11] J.M. Murray, Optimal control for a cancer chemotherapy problem with general growth and loss functions, Math. Biosci. 98 (1990) 273–287.
[12] R. Martin, K.L. Teo, Optimal Control of Drug Administration in Cancer Chemotherapy, World Scientific., 1994.
[13] K.R. Fister, J.C. Panetta, Optimal control applied to cell-cycle-specific cancer chemotherapy? SIAM J. Appl. Math. 60 (3) (2000) 1059–1072.
[14] K.R. Fister, J.C. Panetta, Optimal control applied to competing chemotherapeutic cell-kill strategies? SIAM J. Appl. Math. 63 (6) (2003) 1954–1971.
[15] A.E. Bryson, Y.C. Ho, Applied Optimal Control, Hemisphere Publishing Corporation, 1975.
[16] CVX, MATLAB software for disciplined convex programming, 2015 http://cvxr.com/cvx/.
[17] W.H. Kwon, S. Han, Receding Horizon Control, Springer, 2005.
[18] J.R. Rawlings, D.Q. Mayne, Model Predictive Control: Theory and Design, Nob Hill Publishing, 2009.
[19] M.L. Bell, D.J.N. Limebeer, R.W.H. Sargent, Robust receding horizon optimal control, Comput. Chem. Eng. 20 (Suppl.) (1996) S781–S786.
[20] J.M. Lemos, Nonlinear receding horizon control based on Pontryagin optimum principle, in: Prep. 8th Symp. Nonlinear Control Systems, Bologna, Italy, 2010, pp. 1069–1074.